Hydrothermal syntheses and structures of the uranyl tellurates AgUO2(HTeO5) and Pb2UO2(TeO6)

Jie Ling [a], Matthew Ward [a], Peter C. Burns [a,b,*]

[a] Department of Civil Engineering and Geological Science, University of Notre Dame, Notre Dame, IN 46556, USA
[b] Department of Chemistry and Biochemistry, University of Notre Dame, Notre Dame, IN 46556, USA

ARTICLE INFO

ABSTRACT

Two uranyl tellurates, $AgUO_2(HTeO_5)$ (**1**) and $Pb_2UO_2(TeO_6)$ (**2**), were synthesized under hydrothermal conditions and were structurally, chemically, and spectroscopically characterized. **1** crystallizes in space group $Pbca$, $a=7.085(2)$ Å, $b=11.986(3)$ Å, $c=13.913(4)$ Å, $V=1181.5(5)$ Å^3, $Z=8$; **2** is in $P2(1)/c$, $a=5.742(1)$ Å, $b=7.789(2)$ Å, $c=7.928(2)$ Å, $V=90.703(2)$ Å^3, and $Z=2$. These are the first structures reported for uranyl compounds containing tellurate. The U^{6+} cations are present as $(UO_2)^{2+}$ uranyl ions that are coordinated by O atoms to give pentagonal and square bipyramids in compounds **1** and **2**, respectively. The structural unit in **1** is a sheet consisting of chains of edge-sharing uranyl pentagonal bipyramids that are one bipyramid wide, linked through the dimers of TeO_6 octahedra. In **2**, uranyl square bipyramids share each of their equatorial vertices with different TeO_6 octahedra, giving a sheet with the autunite-type topology. Sheets in **1** and **2** are connected through the low-valence cations that are located in the interlayer region. The structures of **1** and **2** are compared to those of uranyl compounds containing octahedrally coordinated cations.

1. Introduction

The first reported crystal structures of uranyl tellurites, which contain U^{6+} and Te^{4+}, were described for three minerals: cliffordite, $UO_2Te_3O_7$ [1], moctezumite, $Pb(UO_2)(TeO_3)_2$ [2], and schmitterite, UO_2TeO_3 [3]. These rare minerals are from the oxidizied zone of a U deposit at Shinkolobwe, Democratic Republic of Congo, and the oxidized zone of a hydrothermal Au/Te deposit at the Moctezuma mine in Mexico [4]. More recently, 11 hydrothermally synthesized uranyl tellurites have been synthesized and structurally characterized: $Pb_2UO_2(TeO_3)_3$ [5], $K[UO_2Te_2O_5(OH)]$ [6], $Tl_3\{(UO_2)_2[Te_2O_5(OH)](Te_2O_6)\}\cdot 2H_2O$ [6], α-$Tl_2[UO_2(TeO_3)_2]$ [7], β-$Tl_2[UO_2(TeO_3)_2]$ [6], $Sr_3[UO_2(TeO_3)_2](TeO_3)_2$ [6], $Na_8[(UO_2)_6(TeO_3)_{10}]$ [7], $A_2[(UO_2)_3(TeO_3)_2O_2]$ ($A=$K, Rb, Cs) [8], and $K_4[(UO_2)_5(TeO_3)_2O_5]$ [9]. Considerable structural diversity is exhibited by these compounds, which contain structural units consisting of uranyl tellurite chains, sheets, and frameworks.

Whereas Te^{4+} typically occurs in a distorted tetrahedral coordination environment, Te^{6+} normally occurs coordinated by six O atoms in a distorted octahedral arrangement. Tellurate thus presents more binding sites than tellurite, and could potentially give more complex extended structures. The coordination of tellurate to metal centers is unusually strong, which enables it to stabilize high oxidation states of the transition metals in an aqueous solution that can then be crys-

tallized, such as Ru(VI) in $Na_6[RuO_2\{TeO_4(OH)_2\}_2]\cdot 16H_2O$ [10], Os(VI) in $Rb_2Na_4[OsO_2\{TeO_4(OH)_2\}_2]\cdot 18H_2O$ [11], Ag (III), Cu(III), and Au(III) in $Na_5[M\{TeO_4(OH)_2\}_2]\cdot 16H_2O$ ($M=$Ag [10], Cu [12], or Au [13]), Pd(IV) in $Na_8K_2H_4[Pd_2Te_4O_{24}H_2]\cdot 20H_2O$ [14], and Pt(IV) in $K_6Na_4[Pt(OH)_2\{TeO_5(OH)\}_2]\cdot 12H_2O$ [14].

Only one actinide tellurate, $Th(VO_2)_2(TeO_6)(H_2O)_2$ [15], has been reported; in combination with uranyl polyhedra, tellurate should give new structure topologies. Here, we begin to explore the reactions of uranyl nitrate with tellurate under relatively mild hydrothermal conditions, and report the syntheses, crystal structures and characterization of two new uranyl tellurates.

2. Experimental

2.1. Synthesis

$UO_2(NO_3)_2\cdot 6H_2O$ (MV Laboratories, Lot no. P705UA1), H_6TeO_6 (99.5%, Alfa-Aesar), $AgNO_3$ (99.9%, Aldrich), and $Pb(NO_3)_2$ (99.5%, Aldrich) were used as received. Distilled and Millipore filtered water with a resistance of 18.2 MΩ cm was used in all reactions. *While the $UO_2(NO_3)_2\cdot 6H_2O$ used in these experiments contains isotopically depleted U, standard precautions for handling radioactive materials should be followed.*

$AgUO_2(HTeO_5)$ (**1**) and $Pb_2UO_2(TeO_6)$ (**2**) were synthesized by reacting 0.086 g $UO_2(NO_3)_2\cdot 6H_2O$ (0.25 mmol), 0.057 g H_6TeO_6 (0.25 mmol), 0.085 g $AgNO_3$ (0.5 mmol) or 0.115 g $Pb(NO_3)_2$

* Corresponding author at: Department of Civil Engineering and Geological Science, University of Notre Dame, Notre Dame, IN 46556, USA.
   E-mail addresses: pburns@nd.edu, Peter.Burns.50@nd.edu (P.C. Burns).

(0.5 mmol) and 2 ml distilled water under hydrothermal conditions, respectively. Reactants were heated in 23 ml Teflon-lined Parr reaction vessels at 220 °C for nine days. After cooling to room temperature, tiny orange needles of **1** or tiny yellow plates of **2**, as minor products, were found together with a major unidentified fine-grained phase. The difficulty of isolating pure materials precluded quantification of the low yields. An EDS analysis provided Ag/U/Te and Pb/U/Te ratios of 1:1:1 (36%:33%:31%) and 2:1:1 (52%:26%:22%), consistent with the formulae assigned from the crystal structure analyses.

2.2. Crystallographic studies

Single crystals of **1** and **2** were selected using a polarized-light stereomicroscope and were mounted on tapered glass fibers using an epoxy for the X-ray diffraction analysis. A sphere of diffraction data was collected for each compound at 110 K, using a Bruker three-circle X-ray diffractometer equipped with an APEX CCD detector. The data were collected using monochromatic MoKα radiation with a frame width of 0.3° in omega, and a counting time per frame of 10 s. Unit-cell parameters were refined by least-squares techniques, using the Bruker SMART software [16]. The SAINT software [17] was used for data integration including Lorentz, background, and polarization corrections. Empirical absorption corrections were applied using the program SADABS. The SHELXTL version 5 series of programs was used for the solution and refinement of the crystal structures [18]. Selected data collection parameters and crystallographic information are listed in Table 1. Selected interatomic distances of these compounds are listed in Tables 2 and 3. Complete details are provided in Supporting Information.

2.3. Bond-valence analysis

The bond valence sums incident upon each atom in the structures were calculated for U^{6+}—O [19], Te^{6+}—O [19], Ag^+—O [20], and Pb^{2+}—O [20] interactions. The sums are listed in the Supporting Information for **1** and **2**. The calculated sums are in good agreement with the formal valences of U^{6+}, Te^{6+}, Ag^+, and Pb^{2+}.

2.4. Infrared spectroscopy

Infrared spectra were obtained for single crystals of **1** and **2**, using a SensIR technology IlluminatIR FT-IR microspectrometer.

Table 1
Crystallographic data for $AgUO_2(HTeO_5)$ (**1**) and $Pb_2UO_2(TeO_6)$ (**2**).

Formula	$AgUO_2(HTeO_5)$	$Pb_2UO_2(TeO_6)$
Formula mass	585.5	908.01
Crystal system	Orthorhombic	Monoclinic
Space group	Pbca	P2(1)/c
a (Å)	7.085(2)	5.742(1)
b (Å)	11.986(3)	7.789(2)
c (Å)	13.913(4)	7.928(2)
β (°)		90.703(2)
V (Å³)	1181.5(5)	354.6(1)
Z	8	2
λ (Å)	0.71073	0.71073
mu (mm⁻¹)	35.513	74.185
θ (°) range	2.93–27.85	3.55–28.56
ρ_{calcd} (g cm⁻³)	6.583	8.505
S	1.020	1.174
$R(F)$ for $F_o^2 > 2\sigma(F_o^2)$ [a]	0.0404	0.0223
$R_w(F_o^2)$ [b]	0.1030	0.0504

[a] $R(F) = \sum ||F_o| - |F_c|| / \sum |F_o|$.

[b] $R_w(F_o^2) = \left[\sum \left[w(F_o^2 - F_c^2)^2 \right] / \sum wF_o^4 \right]^{1/2}$.

Table 2
Selected interatomic distances (Å) for $AgUO_2(HTeO_5)$ (**1**).

U(1)–O(1)	2.373(9)	Te(1)–O(3)	1.984(10)
U(1)–O(1)	2.246(12)	Te(1)–O(4)	1.896(11)
U(1)–O(2)	1.794(12)	Te(1)–O(6)	1.876(10)
U(1)–O(4)	2.557(10)	Te(1)–O(7)	1.937(11)
U(1)–O(4)	2.318(11)	Ag(1)–O(2)	2.312(11)
U(1)–O(5)	1.770(12)	Ag(1)–O(3)	2.410(10)
U(1)–O(6)	2.308(9)	Ag(1)–O(6)	2.411(11)
Te(1)–O(1)	1.904(10)	Ag(1)–O(7)	2.569(11)
Te(1)–O(3)	1.966(10)	Ag(1)–O(7)	2.862(11)

Table 3
Selected interatomic distances (Å) for $Pb_2UO_2(TeO_6)$ (**2**).

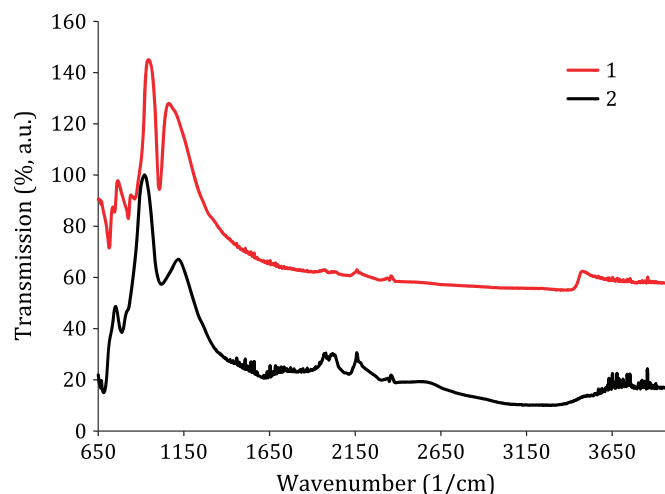| U(1)–O(1) × 2	2.236(7)	Pb(1)–O(1)	2.641(7)
U(1)–O(2) × 2	2.240(7)	Pb(1)–O(2)	2.492(6)
U(1)–O(3) × 2	1.839(6)	Pb(1)–O(3)	2.587(7)
Te(1)–O(1) × 2	1.943(6)	Pb(1)–O(3)	2.906(7)
Te(1)–O(2) × 2	1.949(7)	Pb(1)–O(4)	2.386(6)
Te(1)–O(4) × 2	1.913(6)	Pb(1)–O(4)	2.457(7)
Te(1)–O(4) × 2	1.913(6)	Pb(1)–O(4)	3.005(7)

Fig. 1. Infrared spectra for compounds **1** and **2**.

A single crystal of each compound was placed on a glass slide and the spectrum was collected using a diamond ATR objective. Each spectrum was taken from 650 to 4000 cm⁻¹ with a beam aperture of 100 μm. Infrared spectra are shown in Fig. 1.

2.5. Chemical analysis

Energy dispersive spectroscopy was performed using an LEO EVO 50 scanning electron microscope. Silver, lead, tellurium, and uranium standards were used to calibrate the analysis, and the EDS-derived ratios are within 3% of those provided by the single-crystal X-ray diffraction structure analyses.

3. Results

Compounds **1** and **2,** each contain only one crystallographically unique U^{6+} cation, and it occurs as a typical $(UO_2)^{2+}$ uranyl ion that is slightly bent (178.1°) in **1** and linear in **2**. The U–O_{Ur} (Ur: uranyl) bond lengths range 1.770(12)–1.839(6) Å. The uranyl ion in the structure of **1** is coordinated by five O atoms that are arranged at the

equatorial positions of a pentagonal bipyramid that is capped by the two O atoms of the uranyl ion. The U–O$_{eq}$ (eq: equatorial) bond lengths range 2.246(12)–2.557(10) Å in **1**. In **2**, the uranyl ion is coordinated by four O atoms at the equatorial vertices of a square bipyramid that is capped by the two O atoms of the uranyl ions. The U–O$_{eq}$ bond lengths are 2.236(7) and 2.240(7) Å. One symmetrically distinct Te^{6+} cation occurs in each structure. In both cases, it is coordinated by six O atoms in an octahedral arrangement, with Te^{6+}–O bond lengths ranging 1.876(10)–1.984(10) Å over the two structures.

The structures of compounds **1** and **2** are dominated by sheets of uranyl bipyramids and TeO$_6$ octahedra (Figs. 2 and 3). In **1**, two symmetrically identical TeO$_6$ octahedra share two bridging O atoms, giving a Te$_2$O$_{10}$ dimer. This appears to be the first occurrence of the sharing of an edge between two tellurate octahedral to give a dimer. Within it, the bridging Te–O–Te angles are 100.3(5)° and the Te–(O)$_2$–Te dihedral angle is 180°. On the basis of the bond-valence analysis, the O(7) atom is protonated and the dimer has composition [H$_2$Te$_2$O$_{10}$]$^{6-}$.

Each uranyl pentagonal bipyramid in the structure of **1** shares two of its equatorial edges with two different adjacent bipyramids, resulting in a chain of uranyl bipyramids that extends along [1 0 0] that is one bipyramid wide (Fig. 2a). These chains of bipyramids are linked into a two-dimensional sheet through the dimers of tellurate octahedra, both through the sharing of polyhedral edges and single vertices (Fig. 2a). The resulting sheets are parallel to (0 1 0) and have composition [UO$_2$(HTeO$_5$)]$^-$. Ag$^+$ ions are located between the sheets, where they are bonded to five O atoms with Ag$^+$–O bond
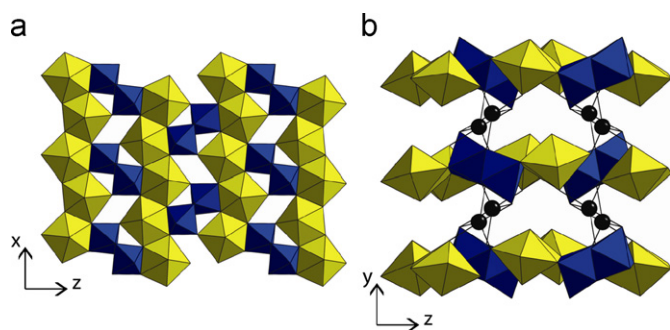

Fig. 2. Polyhedral representations of the structure of compound **1**. (a) The two-dimensional [UO$_2$(HTeO$_5$)]$^-$ sheet projected onto the (0 1 0) plane. (b) The structure projected onto the (1 0 0) plane, showing the stacking of the uranyl tellurate sheets and the interlayer Ag cations. Uranyl and tellurate are shown as yellow and blue polyhedra, respectively. Black spheres represent silver cations.
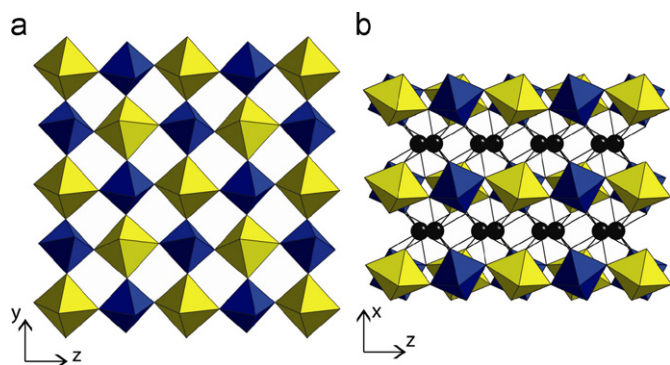

Fig. 3. Polyhedral representation of the structure of compound **2**. (a) The two-dimensional [UO$_2$(TeO$_6$)]$^{4-}$ sheet projected onto the (1 0 0) plane. (b) Projection of the structure onto the (0 1 0) plane, showing the stacking of the uranyl tellurate sheets and the interlayer Pb cations. Uranyl and tellurate polyhedra are shown in yellow and blue, respectively. Black spheres represent Pb cations.

distances varying from 2.31(1) to 2.86(1) Å. Three of these bonds are to the sheet on one side, and extend to an O atom of a uranyl ion, an O atom that is an equatorial vertex of a uranyl pentagonal bipyramid and that is also shared with a TeO$_6$ octahedron, and a non-bridging O atom of a TeO$_6$ octahedron (Fig. 2b). Two bonds extend to the sheet on the other side, linking the Ag$^+$ cation to an O atom that bridges between two TeO$_6$ octahedra, and a non-bridging O atom of a TeO$_6$ octahedron (Fig. 2b).

Each uranyl square bipyramid in compound **2** shares each of its equatorial vertices with four different TeO$_6$ octahedra, and each TeO$_6$ octahedron is linked to four uranyl square bipyramids (Fig. 3). The resulting sheet, which is parallel to (1 0 0), is based on the well-known autunite topology [21] that contains only square sites. Linkages between the sheets are provided by the Pb^{2+} cations. Each O atom of a uranyl ion is bonded to two Pb^{2+} cations with bond lengths ranging 2.587(6)–2.906(7) Å, and each non-bridging O atom of a TeO$_6$ octahedron is bonded to two Pb^{2+} cations with bond lengths of 2.386(6) and 2.457(6) Å. The coordination environment about the Pb^{2+} cations is strongly distorted owing to the presence of a stereoactive lone pair of electrons. There are five shorter bonds to O atoms on one side of the polyhedron, with bond lengths ranging 2.386(6)–2.641(7) Å, and two longer interactions on the other side of the Pb^{2+} cation with interatomic distances of 2.906(7) and 3.005(7) Å.

The infrared spectra of **1** and **2** are similar (Fig. 1). Several sharp bands occurring in the range 800–980 cm^{-1} (941, 895, and 882 cm^{-1} in **1**, 879, 827, and 807 cm^{-1} in **2**) are assigned as asymmetric stretches of the uranyl units. Strong bands at 729 and 710 cm^{-1} in **1**, and 708 cm^{-1} in **2** are attributed to the asymmetric stretching vibrations of Te–O bonds. A weak band at ~3450 cm^{-1} in the spectrum of **1** confirms the presence of H.

4. Discussion

Compounds **1** and **2** are the first uranyl tellurate compounds, and both display interesting structural sheets that are topologically related to those in other uranyl compounds. Octahedrally coordinated cations (other than U^{6+}) are relatively rare in the structural units in uranyl compounds. Five previously reported uranyl compounds contain MoO$_6$ octahedra. Iriginite ([(UO$_2$)Mo$_2$O$_7$(H$_2$O)$_2$](H$_2$O)) [22], and two synthetic uranyl molybdates: [(UO$_2$)Mo$_2$O$_7$(H$_2$O)$_2$] [23] and [Ca(UO$_2$)(Mo$_4$O$_7$)$_2$] [24], contain topologically identical sheets consisting of uranyl pentagonal bipyramids and dimers of MoO$_6$ octahedra that are formed by the sharing of an equatorial edge. These dimers are linked to each other by sharing two vertices with adjacent dimers, giving a chain of octahedra. These chains are linked through the uranyl pentagonal bipyramids. The compounds A_{10}[(UO$_2$)$_8$O$_8$(Mo$_5$O$_{20}$)] (A=Ag, Na) [25] have sheets that contain uranyl pentagonal bipyramids and dimers of edge-sharing MoO$_6$ octahedra. Unlike in compound **1**, the sheets contain chains of uranyl pentagonal bipyramids that are three polyhedra wide; thus, the details of linkages of the chains of bipyramids with the MoO$_6$ octahedra are also unique.

Five uranyl compounds contain WO$_6$ octahedra. Four of these, K$_2$[(UO$_2$)(W$_2$O$_8$)] [26], Na$_2$[(UO$_2$)(W$_2$O$_8$)] [27], α-Ag$_2$[(UO$_2$)(W$_2$O$_8$)] [27], and β-Ag$_2$[(UO$_2$)(W$_2$O$_8$)] [27] are built with a sheet with similarities to that found in compound **1**. The sheet contains chains of edge-sharing uranyl pentagonal bipyramids which are one polyhedron wide. These chains are linked into a sheet through a ribbon of WO$_6$ octahedra formed through the sharing of edges and vertices. The ribbon is two WO$_6$ octahedra wide and is connected to the chains of bipyramids through the equatorial edges of the octahedra. Note that in compound **1**, the TeO$_6$ octahedra are arranged in dimers, rather than as a continuous ribbon. The structure of Cs$_6$[(UO$_2$)$_4$(W$_5$O$_{21}$)(OH)$_2$(H$_2$O)$_2$] [28] contains rather complex sheets of uranyl pentagonal bipyramids and both WO$_6$ octahedra and WO$_5$ square pyramids. In this

sheet, the pentagonal bipyramids are linked into four-membered rings, with a WO_5 square pyramid located at the center of the ring. These units are further linked into a sheet through the dimers of edge-sharing WO_6 octahedra.

The compounds $[(UO_2)TiNb_2O_8]$ [29], $[(UO_2)Nb_3O_8]$ [30], and $Cs[UV_3O_8]$ [31] contain topologically identical sheets with uranyl hexagonal bipyramids linked by sharing edges with TiO_6, NbO_6 or VO_6 octahedra. The uranyl bipyramids are not directly linked within the sheet.

The sheet of uranyl square bipyramids and TeO_6 octahedra in **2** is based on the autunite anion topology that consists only of squares. The connectivity of this net is 4.4.4.4 [32]. In the autunite group of minerals, uranyl square bipyramids are connected through phosphate tetrahedra, such that each tetrahedron is linked to four different square bipyramids. Several synthetic compounds have topologically identical sheets with arsenate tetrahedra, rather than phosphate. Several compounds contain sheets of equatorial-vertex sharing uranyl square bipyramids that also exhibit the same anion topology. Compound **2** is the first to contain sheets based on the autunite topology that contain octahedra (other than U^{6+}). It is interesting that several compounds contain uranyl phosphate sheets with the autunite topology, with lower-valence octahedrally coordinated cations in the interlayer positions (i.e., Al, Mg, Cu).

In summary, compounds **1** and **2**, the first reported uranyl tellurates, present structures that are unique, but that have features in common with other uranyl compounds. Consistent with the majority of uranyl compounds, their structural units are sheets, with lower-valence cations located between the sheets. Continued exploration of the uranyl-tellurate system may reveal additional interesting structural topologies.

Supporting information

Supporting information includes crystallographic information files (CIFs) for compounds **1** and **2**, as well as a bond-valence analysis for each compound.

Acknowledgment

Appendix A. Supporting information

Supplementary data associated with this article can be found in the online version at doi:10.1016/j.jssc.2010.12.007.

References

[1] R.V. Gaines, Mineral. Rec. 1 (1970) 40.
[2] R.V. Gaines, Am. Mineral. 54 (1969) 697.
[3] R.V. Gaines, Univ. Nacl. Auton. Mex., Inst. Geol. Biol. 75 (1965) 1.
[4] J.W. Anthony, R.A. Bideaux, K.W. Bladh, M.C. Nichols, Handbook of Mineralogy, Volume V, Borates, Carbonates, Sulfate, Mineral Data Publishing, Tuscon, 2003 vol. 5.
[5] F. Branstätter, Z. Kristallogr. 155 (1981) 193.
[6] P.M. Almond, T.E. Albrecht-Schmitt, Inorg. Chem. 41 (2002) 5495.
[7] P.M. Almond, M.L. Mckee, T.E. Albrecht-Schmitt, Angew. Chem., Int. Ed. 41 (2002) 3426.
[8] J.D. Woodward, P.M. Almond, T.E. Albrecht-Schmitt, J. Solid State Chem. 177 (2004) 3971.
[9] J.D. Woodward, T.E. Albrecht-Schmitt, J. Solid State Chem. 178 (2005) 2922.
[10] A.L. Hector, N.J. Hill, W. Levason, M. Webster, Z. Anorg. Allg. Chem. 628 (2002) 815.
[11] W. Levason, R.D. Oldroyd, M. Webster, J. Chem. Soc., Dalton Trans. 20 (1994) 2983.
[12] W. Levason, M.D. Spicer, M. Webster, J. Chem. Soc., Dalton Trans. 5 (1988) 1377.
[13] W. Levason, M. Webster, Acta Crystallogr. C54 (1998) 1729.
[14] W. Levason, M.D. Spicer, M. Webster, Inorg. Chem. 30 (1991) 967.
[15] T.A. Sullens, T.E. Albrecht-Schmitt, Inorg. Chem. 44 (2005) 2282.
[16] A.X.S. Bruker, SMART, Bruker AXS, Madison, MI, 1998.
[17] A.X.S. Bruker, SAINT, Bruker AXS, Madison, MI, 1998.
[18] G.M. Sheldrick, SHELTXL, Bruker A.X.S., Madison, WI, 1996 version 6.12.
[19] P.C. Burns, Can. Mineral. 43 (2005) 1839.
[20] N.E. Brese, M. O'Keeffe, Acta Crystallogr. B47 (1991) 192.
[21] A.J. Locock, P.C. Burns, Am. Mineral. 88 (2003) 240.
[22] S.V. Krivovichev, P.C. Burns, Can. Mineral. 38 (2000) 847.
[23] S.V. Krivovichev, P.C. Burns, Can. Mineral. 40 (2002) 1571.
[24] M.R. Lee, S. Jaulmes, J. Solid State Chem. 67 (1987) 364.
[25] S.V. Krivovichev, P.C. Burns, Can. Mineral. 41 (2003) 1455.
[26] S. Obbade, C. Dion, E. Bekaert, S. Yagoubi, M. Saadi, F. Abraham, J. Solid State Chem. 172 (2003) 305.
[27] S.V. Krivovichev, P.C. Burns, Solid State Sci. 5 (2003) 373.
[28] R.E. Sykora, T.E. Albrecht-Schmitt, J. Solid State Chem. 177 (2004) 3729.
[29] R. Chevalier, M. Gasperin, C. R. Acad. Sci. C268 (1969) 1426.
[30] R. Chevalier, M. Gasperin, C. R. Acad. Sci. C267 (1968) 481.
[31] I. Duribreux, C. Dion, F. Abraham, M. Saadi, J. Solid State Chem. 146 (1999) 258.
[32] P.C. Burns, M.L. Miller, R.C. Ewing, Can. Mineral. 34 (1996) 845.